

# NO<sub>2</sub>-Based Laser-Induced Fluorescence Technique to Measure Cold-Flow Mixing

A. Gulati\* and R. E. Warren Jr.\*

*General Electric Company, Schenectady, New York 12301*

The technique of NO<sub>2</sub>-based laser-induced fluorescence (LIF) for the study of cold flow mixing is extended to high-pressure applications by detailed investigations of its sensitivity and resolution capabilities in well-calibrated fuel-air mixtures of known NO<sub>2</sub> concentration at pressures of up to 10 atm. Effects of pressure and mixture composition on the fluorescence signal are examined and it is shown that quenching effects can be accounted for with the appropriate calibration process. At atmospheric pressure conditions the technique has excellent dynamic range (1:500). The dynamic range reduces at elevated pressures. Plausible explanations for the observed nonlinear deviation of signal with pressure are presented. The absolute upper pressure limit for the applicability of the technique is estimated to be 14 atm. Various issues involved in rendering the technique practical for application to full-scale premixers are discussed. Finally, the technique is applied to the study of mixing of a turbulent jet issuing into coflowing air where it is shown that the technique can resolve partially mixed small scale eddies with excellent spatial and temporal resolution.

## I. Introduction

WITH the increased concern about environmental pollution introduced by power-generating equipment such as land-based gas turbines and aircraft engines, there has been a significant increase in the effort to lower the emission levels of such powerplants. Two of the major pollutants in the exhaust of these powerplants have been identified as CO and the oxides of nitrogen (called NO<sub>x</sub>). One of the primary routes NO<sub>x</sub> is produced in conventional powerplants (which to date have been mostly of the diffusion type) is thermal,<sup>1</sup> i.e., conversion of atmospheric N<sub>2</sub> to nitrogen-oxides at the peak temperatures obtained at the stoichiometric mixing contours typical of diffusion flames. There is, therefore, an increased interest in changing the mode of combustion to what is termed lean premixed combustion, which results in much lower levels of thermal NO<sub>x</sub>. The new designs of combustors being developed are mainly of this type in one form or the other. These new combustors are typically divided into two sections: 1) a fuel-air premixing section termed "premixer" and 2) a combustion section where the lean premixed mixture is burned. An important issue that has emerged in the design of these low NO<sub>x</sub> combustors is the effectiveness of the premixing section. Initial tests of lean premixed combustion have shown that the window of equivalence ratios over which low NO<sub>x</sub> is produced is fairly narrow,<sup>2</sup> and the increase of NO<sub>x</sub> emissions with increased equivalence ratio is both dramatic and nonlinear. The nonlinear increase of NO<sub>x</sub> emissions with equivalence ratio strongly suggests that even small pockets of poorly mixed fuel/air could have a dramatic effect on the NO<sub>x</sub> performance. Thus, not only is it important to obtain good premixing in the premixer on the average, but it is also important that the local temporal excursions of the mixture fraction from the desired mean value be minimal.

Current conventional means to measure the effectiveness of such premixers are limited to probe-sampling techniques based on detection of hydrocarbons and other such species

introduced into the fuel stream as a marker. Besides perturbing the flow and having less than adequate spatial resolution, probe-sampling techniques, however, are mostly time-averaging techniques, and thus suffer from a major drawback of being unable to resolve any temporal fluctuations in the fuel-air mixture fraction values. As previously discussed, it is believed that such excursions from the designed mean mixture fraction values could have a significant impact on the NO<sub>x</sub> emissions of the combustor. There is, therefore, an urgent need to develop an alternative means of measuring mixture concentration with adequate temporal and spatial resolution to resolve this issue and to provide a tool to evaluate the effectiveness of practical premixing configurations being developed.

In the past, a number of techniques based on laser spectroscopy<sup>3,4</sup> have been developed and applied in various systems. Laser-induced fluorescence is a common technique used to probe the flowfield to measure various species of interest. Another application of laser-induced fluorescence is to study mixing in various flowfields, such as in a subatmospheric supersonic stream<sup>5</sup> based on laser-induced fluorescence from iodine (PLIIF) which is seeded in the fuel stream as a marker. PLIIF and other techniques, however, have considerable limitations, e.g., iodine fluorescence signal drops significantly at atmospheric and higher pressures because of increased quenching.<sup>6</sup> Moreover, it is difficult to control the seeding rate of iodine introduced into the fuel stream. In an earlier paper, Agarwal et al.<sup>7</sup> have reported on preliminary measurements of an NO<sub>2</sub>-based fluorescence technique to measure mixing in an atmospheric pressure-type application. However, their study was not extended further and not much work has been done in exploiting this technique to measure fuel-air mixing in practical systems. In this article we present recently obtained results that extend the capabilities of the NO<sub>2</sub>-based fluorescence technique to high-pressure systems. We also apply the technique to the study of mixing of a turbulent jet issuing in coflowing airstream at atmospheric pressure. Finally, we address some of the issues involved in applying this technique to the evaluation of practical premixing systems. In Sec. II we present briefly the principle of the LIF technique. Section III describes some of the experimental details. Results are presented in Sec. IV.A and IV.B. in well-calibrated fuel-air mixtures at various pressures to determine the sensitivity and spatial resolution of the technique, and Sec. IV.C. downstream of a turbulent jet issuing in coflowing

Presented as Paper 92-0511 at the AIAA 30th Aerospace Sciences Meeting, Reno, NV, Jan. 6-9, 1992; received Oct. 8, 1992; revision received Feb. 23, 1993; accepted for publication March 26, 1993. Copyright © 1993 by the American Institute of Aeronautics and Astronautics, Inc. All rights reserved.

\*Aeronautical Engineer, Corporate Research and Development Laboratory. Member AIAA.

airstream to demonstrate the temporal capabilities of the technique. Section V discusses some of the issues involved in the practical implementation of the technique.

## II. Laser-Induced Fluorescence

The principle of the technique is relatively straightforward and is discussed briefly here. For details the reader is referred to a number of excellent books<sup>3</sup> and papers on the general topic of laser diagnostics. As in all fluorescence techniques, a particular species of interest is chosen (in this case NO<sub>2</sub>) and is either seeded in one of the streams as a marker or is produced in the region of interest and probed with a laser beam at the appropriate wavelength. The resultant "fluorescence" signal is then used to obtain information about the composition of the gas and its state. The advantages of NO<sub>2</sub> as a marker are numerous: 1) its absorption cross section contains many lines in the visible spectrum readily accessible with conventionally available CW lasers (argon-ion laser), 2) its cross section is fairly large, and the resulting fluorescence signal is easily measurable, 3) its fluorescence signal is red-shifted and fairly broadband so that a sharp cutoff filter can eliminate background scattered light, 4) the quenching effects (to be discussed later) are not that severe and are interpretable at least in the range of conditions of interest here, and finally, 5) NO<sub>2</sub> is readily available in gaseous form in well-calibrated mixtures with N<sub>2</sub> and air, is noncorrosive, stable, and has a molecular weight of 46, which is not very different from that of air; thus the NO<sub>2</sub> introduced into the fuel stream as marker should mix well at a molecular level and should track it faithfully at the high Reynolds number flows of interest here. The major disadvantage of NO<sub>2</sub> is that it is toxic, and therefore, significant precautions have to be taken in its applications. This issue is discussed in detail later.

The physics of the processes involved in the generation and interpretation of the fluorescence signal can be understood as follows: in general, when coherent laser light interacts with molecules of gaseous species in the probe volume, three types of interactions occur: 1) absorption, 2) emission, and 3) scattering. The best way to think of fluorescence is as a two-step process, namely, rapid energy absorption followed by rapid emission. Figure 1 shows a simplified version of the interaction that takes place when laser light interacts with molecules of NO<sub>2</sub> in the gaseous mixture. Spontaneous emission represented by *A* in Fig. 1 is termed fluorescence. In the presence of other molecules in the probe volume, however, another energy exchange termed quenching *Q* also occurs that competes with the fluorescence signal and renders its interpretation more difficult. The effect of quenching will be discussed in more detail later.

One of the major advantages of fluorescence as opposed to light-scattering processes such as Rayleigh scattering is that the signal is frequency shifted and occurs mostly at higher

wavelengths. The practical implication is that with the use of appropriate cutoff filters most spurious light scattered from windows, which would otherwise contaminate the signal, can be eliminated. NO<sub>2</sub>, being a complex molecule, absorbs light over a wide range of wavelengths in the visible spectrum. In this study we have chosen the 488.0-nm line of a continuous wave argon-ion laser to excite the NO<sub>2</sub> molecule, since it is one of the strongest lines available and overlaps many lines of the NO<sub>2</sub> absorption spectra. The emission occurs in two main bands from 655 to 625 nm and from 605 to 560 nm. We measured all broadband emission over 550 nm in this study.

Equation (1) is a general equation relating the collected fluorescence signal to the concentration of NO<sub>2</sub> molecules in the probe volume:

$$I_f = \frac{I_i \eta \Omega N_a A}{(A + Q)} \quad (1)$$

In the above equation, *I<sub>f</sub>* is the measured fluorescence signal, *I<sub>i</sub>* the incident laser energy, *η* the collection efficiency, *l* the length of the probe volume measured, *Ω* the solid angle of the optics, *N<sub>a</sub>* the population density of molecules of NO<sub>2</sub> with absorption spectra coinciding with the 488.0-nm light of the argon-ion laser, *A* the net spontaneous emission rate of the excited states, and *Q* the collisional quenching rate. From Eq. (1) it is clear that the signal is linearly proportional to the number density (concentration) of NO<sub>2</sub> molecules if all else remains constant. The term most difficult to predict in Eq. (1) is *Q*, the quenching rate caused by collisions with other species in the probe volume. Quenching affects the interpretation of the signal since it is, in general, a function of the temperature and pressure of the gas and its composition. Some of the experiments conducted here will show the dependence of quenching on the composition of the gas and pressure.

Further examination of Eq. (1) reveals other important features of the technique, some of which are later examined experimentally: 1) the fluorescence signal varies linearly with laser power—an important test to distinguish the technique from saturated fluorescence, 2) the signal is directly proportional to the length of the probe volume *l*, which also determines the spatial resolution of the technique. Finally, Eq. (1) shows that the signal is directly proportional only to the number density of molecules in the population states being excited by the laser. However, since the argon-ion laser being used here overlaps a number of lines (up to 100) of the absorption spectra of NO<sub>2</sub>, minor shifts in population densities of various states are averaged out, and it can be shown that the signal is indeed proportional to the quantity of interest, viz., the overall number density *N*. Finally, in Eq. (1) the remaining parameters, e.g., *η* and *Ω*, are all lumped into a constant which is then determined by experimental calibration.

## III. Experimental Setup

Figure 2 shows a schematic of the experimental setup used. The laser beam from the 4.0-W spectra physics argon-ion laser is focused by a 120-mm-focal length lens forming the probe volume. The fluorescence scattered light is collected by a f2.4, 120-mm-focal length lens, collimated, filtered using a Melles-Griot sharp cutoff high pass filter (cutoff wavelength = 550.0 nm), and then focused onto an RCA 4526 photomultiplier tube (PMT) after passing through a 2.0 × 0.5-mm entrance slit. The slit is aligned such that the length of the probe volume in the direction of propagation of the laser beam is 2.0 mm. The choice of the filter is optimized to allow the maximum fluorescence signal to pass through with minimum contamination from the scattered laser light. The RC time constant of the PMT is selected to provide adequate temporal resolution (20 kHz). The signal from the PMT is low-pass filtered (0–20 kHz), amplified (Tektronix AM502 amplifier), digitized at 20 kHz with a 12-bit 50-kHz DT2821 data translation

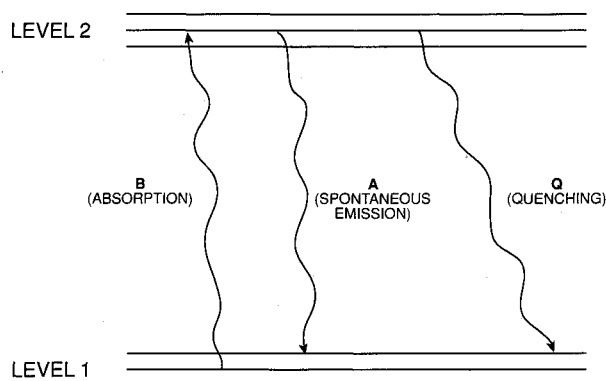


Fig. 1 Simplified schematic showing the energy transitions involved in laser-induced fluorescence spectroscopy.

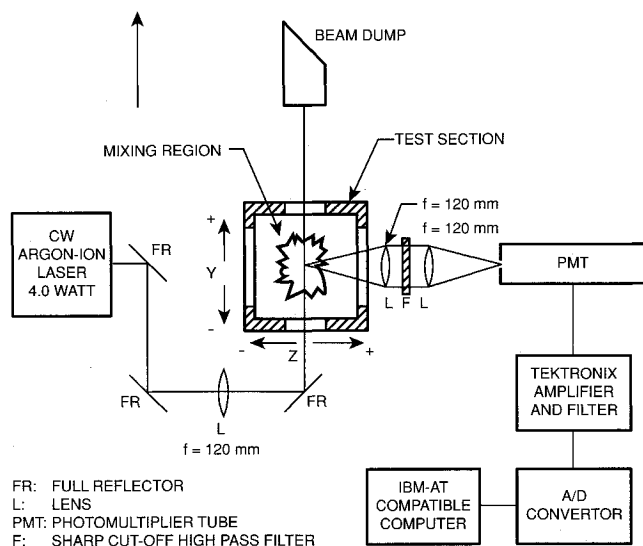


Fig. 2 Schematic of the experimental setup.

board and acquired by a Dell 310 IBMAT-based microcomputer and stored for further processing. Typically, 5000 data points are recorded at every location in less than a second.

The test section consists of a 150- × 150-mm wind tunnel with quartz windows on all sides to provide adequate optical access. The walls of the test section are painted black to absorb light scattered from windows. Two separate tests were conducted. The first set of tests was conducted in a 100- × 100-mm high-pressure cell mounted inside the tunnel to check for sensitivity and linearity of the technique at various pressures in the range of 0–10 atm. Well-calibrated bottles of NO<sub>2</sub> in N<sub>2</sub> mixtures in the range of 10–10,000 ppm were used to obtain good quality data. In some cases, the NO<sub>2</sub> mixture was diluted with other gases such as O<sub>2</sub>, N<sub>2</sub>, air, and CH<sub>4</sub>, to determine the relative effect of quenching, if any, on the fluorescence signals. The second set of tests was conducted to demonstrate the temporal resolution of the technique by studying the mixing of a turbulent jet issuing into coflowing air. The Reynolds number of the jet was 2000. Radial profiles at two axial planes downstream of the jet were obtained to determine the mean and rms profiles of concentration and its pdf at these locations. Time traces of the variation of fuel concentration at typical locations in the mixing region were also obtained. Power spectra based on these time traces were used to resolve the spectral content of the data at up to 10 kHz based on the data acquisition rate of 20 kHz.

#### IV. Results

##### A. Static Tests

The results presented in this section are obtained in a static pressure test cell in which a well-calibrated mixture of NO<sub>2</sub> in N<sub>2</sub> was introduced, and the resulting fluorescence signal was measured as a function of various parameters. These tests were used to determine the spatial and temporal resolution and the sensitivity (dynamic range) of the technique. Figure 3 shows a typical signal trace obtained with a 1.0-W argon-ion laser with a 2000-ppm NO<sub>2</sub> in N<sub>2</sub> mixture using the experimental setup depicted in Fig. 2. As can be seen, the signal is fairly constant, and the measured fluctuations are less than 1.5%. This value is approximately twice the value estimated on the basis of photon flux and associated quantum efficiencies, and is believed to be due to random fluctuations in the power level of the argon-ion laser. The background signal obtained with pure N<sub>2</sub> is also shown for reference and is seen to be negligible. Typical signal to background ratio at this seeding rate is 30:1. This ratio goes down with the seeding level, the worst case being at a seeding rate of 10 ppm of approximately 2:1. The background signal is a function of the

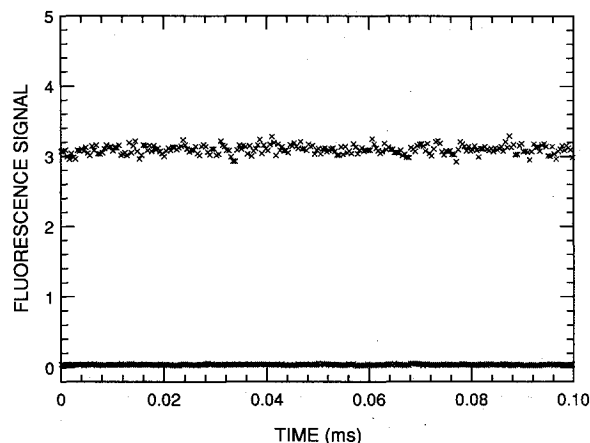


Fig. 3 Typical fluorescence signal trace obtained with a 2000 ppm of NO<sub>2</sub> in N<sub>2</sub> mixture at atmospheric pressure. Background signal obtained with pure N<sub>2</sub> is also shown for reference. Laser power = 1.0 W.

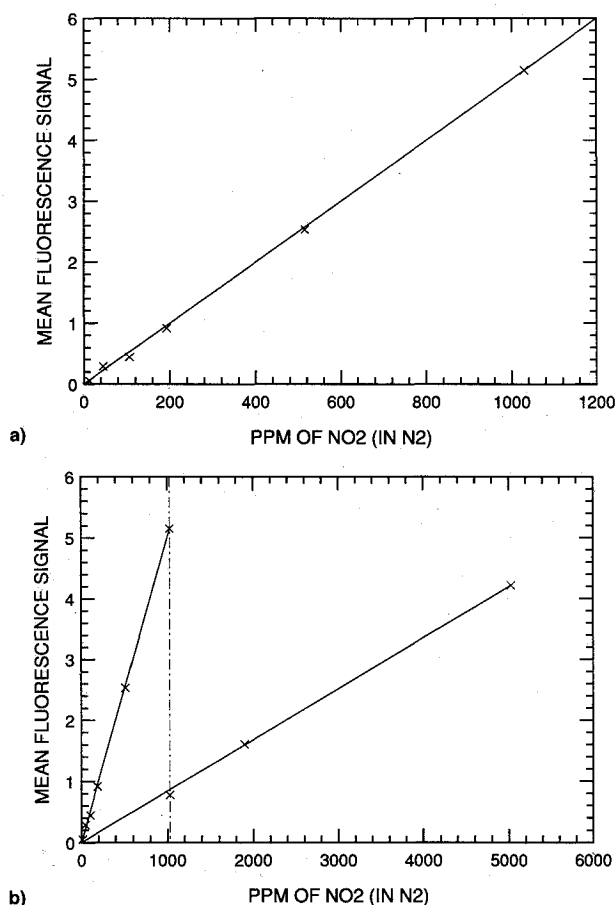


Fig. 4 Variation of the fluorescence signal with concentration of NO<sub>2</sub> in N<sub>2</sub> at atmospheric pressure: a) 0–1200 ppm and b) 0–5000 ppm.

optics, reflectivity of walls of the test section, etc., and can be subtracted at every location by measuring it separately with pure N<sub>2</sub>/airflow. In the rest of the results presented here, the data is always shown with the mean background signal subtracted out. The variation of the mean signal with the concentration of NO<sub>2</sub> in N<sub>2</sub> (in ppm) is shown in Fig. 4. The minimum sensitivity of the technique is 10 ppm. Figure 4 shows that the signal is linear throughout the range of 10–5000 ppm tested, and the dynamic range of the technique at this seeding rate is approximately 1:500. The dynamic range reduces at decreased seeding rates. This dynamic range is much larger than that reported by Agarwal et al.<sup>7</sup> where they had reported leveling off of the signal for concentration greater

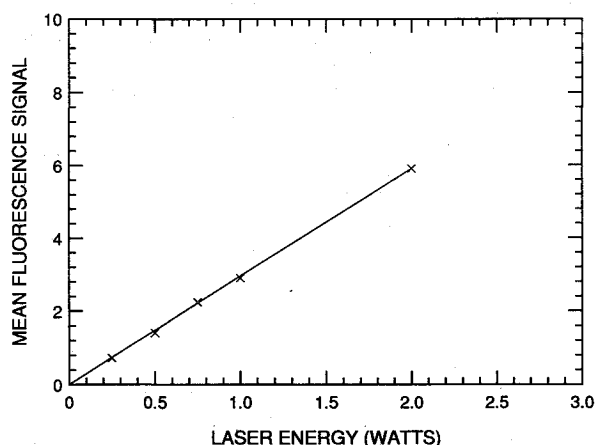


Fig. 5 Variation of the fluorescence signal with laser power of the 488.0-nm line of argon-ion laser for a 1000-ppm NO<sub>2</sub> mixture at atmospheric pressure.

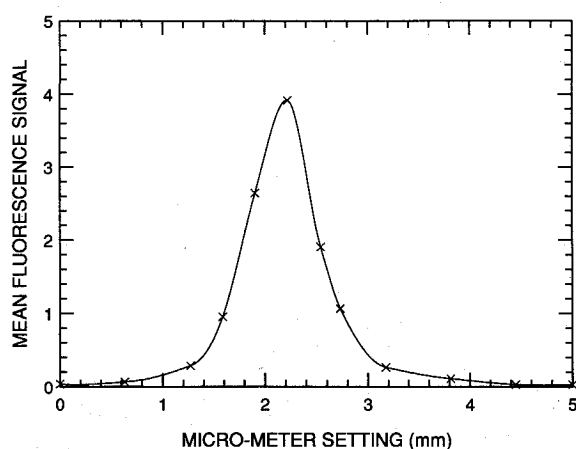


Fig. 6 Profile of the fluorescence signal obtained by scanning across the laser beam for the same conditions as in Fig. 3.

than 500 ppm. A possible explanation for their low dynamic range is the saturation of some component of their measurement system. Figure 5 shows the variation of the signal strength with laser power in the range of 0–2 W for a concentration of 1000 ppm of NO<sub>2</sub>. The signal is linear up to the maximum available power of 2.0 W in the 488.0-nm line of the laser showing that the fluorescence signal is not saturated and that we are operating in the linear fluorescence regime in which Eq. (1) is applicable.

The spatial resolution of the technique is determined by scanning across the path of the laser beam with a slit of fixed width and height ( $0.5 \times 2.0$  mm). As Fig. 6 shows, the curve is a typical Gaussian representative of the Gaussian intensity profile of the laser beam. It has a full-width at half of maximum (FWHM) of approximately 0.75 mm. The beam diameter at the waist is calculated to be 250  $\mu$ m, which is much smaller than the slit width and represents the maximum achievable transverse resolution. The spatial resolution along the direction of the beam is set by the height of the slit (2.0 mm) and by the magnification ratio of the optics, which in this case is approximately 1:1. One way of improving the spatial resolution in the direction of laser beam would be to decrease the slit height and to increase the laser power.

Another important issue examined in these tests is the effect of carrier gas, if any, on the quenching of the fluorescence signal. To study this effect, a 1000-ppm mixture of NO<sub>2</sub> in N<sub>2</sub> was diluted with various gases (1:1 by volume), and the resulting fluorescence signals were recorded. The results show that the signal is independent of the carrier gas as long as it is diatomic, e.g., N<sub>2</sub>, O<sub>2</sub>, H<sub>2</sub>, or air. However, for the mixture

seeded with CH<sub>4</sub>, the signal is 33% lower, which is believed to be due to the increased quenching cross section offered by the much larger CH<sub>4</sub> molecules. These results are corroborated by the reported<sup>8,9</sup> quenching rate constants of  $3.1 \times 10^{-11}$  cm<sup>3</sup>/mole/s for N<sub>2</sub>,  $3.4 \times 10^{-11}$  cm<sup>3</sup>/mole/s for O<sub>2</sub>, and  $7.4 \times 10^{-11}$  cm<sup>3</sup>/mole/s for CO<sub>2</sub>, which is a larger molecule. Similarly, the signal is approximately 30% higher with helium because the helium atom offers a smaller cross section and reduced quenching. The practical implication of these results is that the interpretation of the fluorescence signal with methane or helium as carrier gas for NO<sub>2</sub> would be more complicated because of the nonlinear variation of the fluorescence signal with the composition of the fuel-air mixture. On further examination, results obtained with methane as carrier gas (not shown here) show that even though, as expected, the fluorescence signal varies with fuel concentration in a nonlinear manner, the resulting curve is single valued, and therefore, can be used to interpret the fluorescence signal in terms of the fuel-fraction in the mixture in an unambiguous manner.

### B. Effect of Pressure

Most practical combustors operate at elevated pressures, therefore, a series of tests was conducted to determine the effect of pressure on the fluorescence signal, if any. Figure 7 shows the effect of varying the concentration of NO<sub>2</sub> (in N<sub>2</sub>) on the fluorescence signal at elevated pressures of  $4.13 \times 10^5$  N/m<sup>2</sup> (4.08 atm) and  $1.033 \times 10^6$  N/m<sup>2</sup> (10.2 atm). The curve obtained at atmospheric pressure (Fig. 4a) is also shown for reference. Figure 7 shows that unlike at atmospheric pressure, at elevated pressures the signal does not vary linearly with concentration of NO<sub>2</sub> and the range of concentrations over which the signal is linear decreases rapidly; e.g., at 4.08 atm (Fig. 7a) the signal is linear in the range 0–600 ppm, whereas at 10.2 atm it is linear only over 0–300 ppm. This deviation

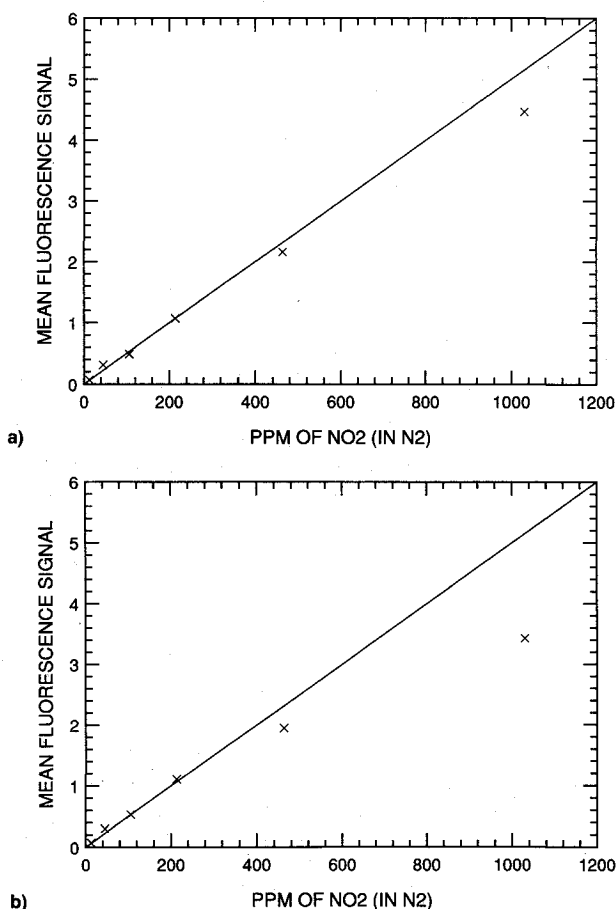


Fig. 7 Variation of the fluorescence signal with concentration of NO<sub>2</sub> in N<sub>2</sub> at elevated pressures of: a) 4.08 atm and b) 10.2 atm.

from nonlinearity increases with pressure and is believed to be due to increased self-quenching. For the case of NO<sub>2</sub>, the self-quenching cross section is reported<sup>8,9</sup> to be  $7.1 \times 10^{-11}$  cm<sup>3</sup>/mole/s which is twice the quenching cross section with N<sub>2</sub>. Therefore, at increased concentrations of NO<sub>2</sub> at elevated pressures, the increase in fluorescence signal could be less than the corresponding increase in self-quenching, resulting in overall drop in the fluorescence signal. This deviation from linearity does not represent a serious limitation of the technique as long as the curve relating the fluorescence signal to the mixture concentration has a positive slope and is single-valued (albeit nonlinear) as shown in Figs. 7a and 7b. The data, however, suggests the upper limit of applicability of the technique to be no more than  $1.4 \times 10^6$  N/m<sup>2</sup> (15 atm).

Another way of examining the effect of pressure is to consider the data of Fig. 8 which shows the measured fluorescence signal level for four seeding levels of NO<sub>2</sub> (in N<sub>2</sub>) of 45, 214, 463, and 1030 ppm as a function of pressure. At low concentrations up to 200 ppm, the signal is, as expected, independent of pressure since the increase in signal strength is accompanied by an equal increase in quenching. At 463 ppm there is a minimal drop with pressure, whereas, at 1030 ppm the signal drops by as much as 30%. This drop in signal is related to the nonlinear behavior of Fig. 7, and is at present not understood well since the increase in self-quenching at elevated pressures could be compounded by other effects such as self-absorption of NO<sub>2</sub> fluorescence, line broadening, and shifting, etc. Fluorescence trapping, i.e., self-absorption cannot explain all the drop in signal in Fig. 8 either. This is because at 1 atm and 5000 ppm (Fig. 4) the amount of NO<sub>2</sub> in the optical path should be approximately the same as that at, e.g., 4.08 atm and 1030 ppm (Fig. 8; third data point of top curve), and therefore, the amount of self-absorption, if any, should be comparable. The data of Fig. 4, however, shows perfectly linear variation of the signal at up to 5000 ppm, whereas the data of Fig. 8 shows a drop of 13% at 4.08 atm (at 1030 ppm). Further work needs to be done to resolve this issue and explain the nonlinear behavior of the data of Fig. 7 and the drop in signal with pressure at the higher seeding levels in Fig. 8.

### C. Turbulent Mixing of Jet

All the results reported thus far were obtained in well-calibrated mixtures of NO<sub>2</sub> of known concentration. To demonstrate the temporal resolution of the technique, it was applied to the study of mixing downstream of a turbulent jet issuing in coflowing air. The jet consists of an 8-mm-diam nozzle and is issuing in coflowing air at a velocity of 5 m/s. The jet velocity is also 5 m/s and corresponds to a Reynolds number of 2000 based on the jet diameter. The jet is supplied with a mixture of NO<sub>2</sub> in N<sub>2</sub> of 1000-ppm concentration.

Radial profiles of the mixture concentration have been obtained at two axial planes downstream of the jet;  $X/a = 1$

and 20. Figure 9 shows the mean concentration profile at  $X/a = 1$ . At this plane the mean profile (normalized by the centerline value) shows a typical Gaussian profile expected of a jet issuing into coflowing air.<sup>10</sup> The rms turbulent profile of the fuel-fraction concentration at the corresponding locations is shown in Fig. 10. The profile shows a peak value of 30% turbulent intensity at  $Y/a = 1$  ( $a$ : the radius of the jet) and vanishing values at the centerline and the edges of the jet corresponding to pure fuel and pure air, respectively. The peak of the curve corresponds to the center of the shear layer where the mixing is most intense. This profile could not have been obtained with any conventional probe-sampling technique.

Figure 11 shows typical traces of the concentration measured at various  $Y/a$  locations in the mixing layer region at  $X/a = 1$ . At the center of the jet ( $Y/a = 0$ ) the signal trace is constant corresponding to the pure jet fluid there (NO<sub>2</sub> in N<sub>2</sub>). Similarly, at the extreme edge of the jet ( $Y/a = 2$ ) the signal is zero corresponding to mostly pure air. For the radial locations in between, as the jet is traversed from the centerline towards the outer edges, an increased amount of air (represented by extremely low values of the signal) is observed. Inside the shear layer, turbulent eddies containing partially premixed fuel and air are present for a significant amount of time and are interspersed with pure fuel and pure air eddies as evident from the trace at  $Y/a = 1.0$ . As the radial distance from the centerline is increased, there is a gradual transition of the concentration from that of mostly fuel with minimal air to the case with mostly coflowing air as expected, based on the mean concentration profile of Fig. 9. This set of traces clearly shows that the NO<sub>2</sub>-based fluorescence technique can

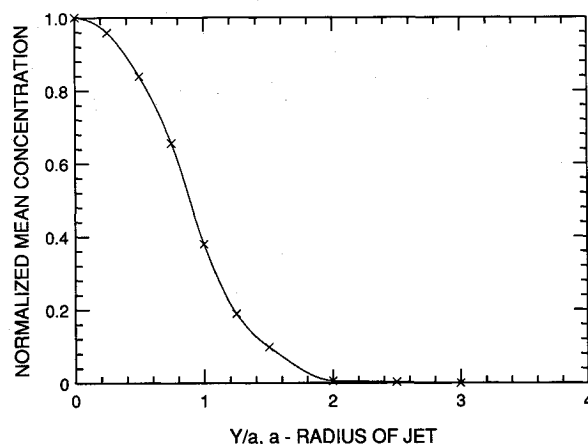


Fig. 9 Profile of mean fuel-air mixture fraction across a turbulent jet mixing in coflowing air at  $X/a = 1$ .

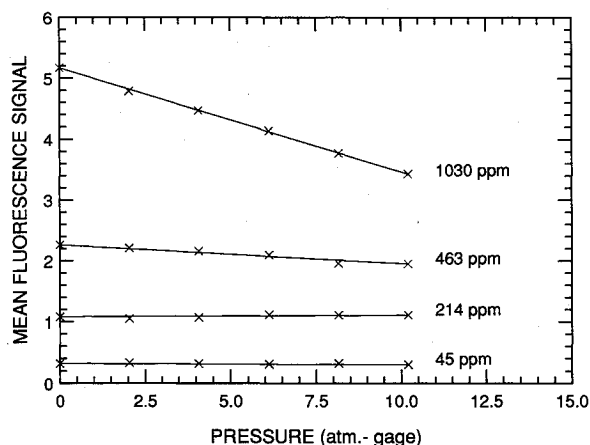


Fig. 8 Effect of variation of pressure on the fluorescence signal for four concentration levels of NO<sub>2</sub> of 45, 214, 463, and 1030 ppm.

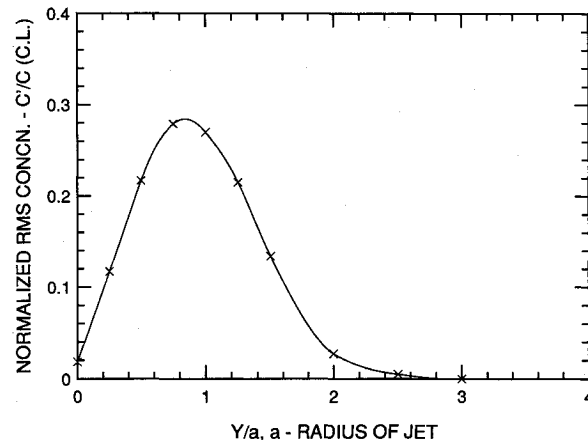


Fig. 10 Profile of rms variation of fuel-air mixture fraction across the turbulent jet mixing in coflowing air at  $X/a = 1$ .

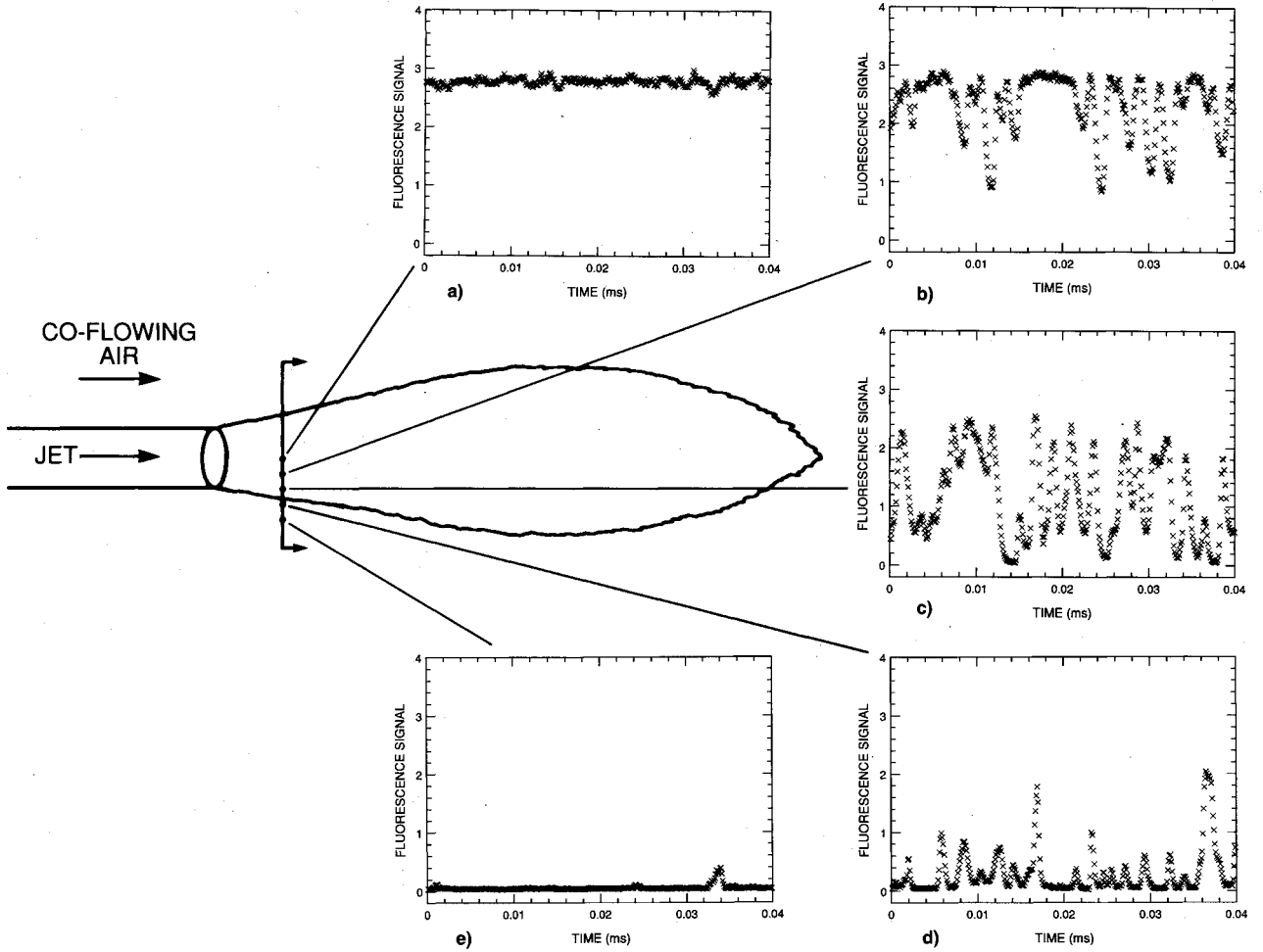


Fig. 11 Measured time traces of the fluorescence signal showing mixing of fuel and air in a time-resolved manner at various locations in the mixing layer region at  $X/a = 1$ ; data taken at 20 kHz;  $Y/a =$  a) 0, b) 0.5, c) 1.0, d) 1.5, and e) 2.0.

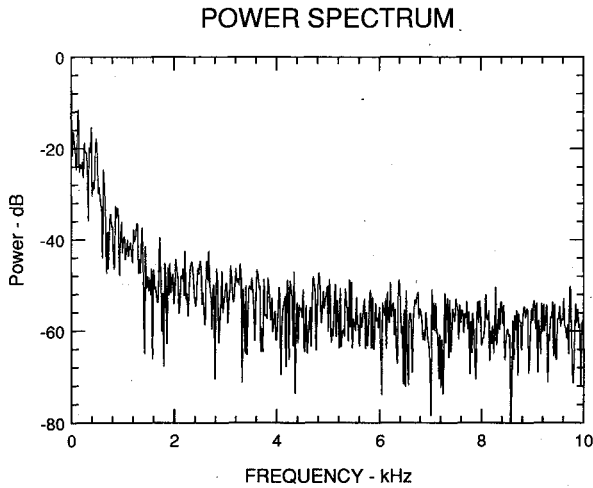


Fig. 12 Power spectrum obtained from the time-resolved fluorescence signal at  $Y/a = 1$ ,  $X/a = 1$  location.

detect small-scale fluctuations in fuel-air mixture ratios in the probe volume, which is not possible with conventional probe sampling techniques. Figure 12 shows a typical frequency spectra of the concentration trace of the signal at  $Y/a = 1$ . Three relative peaks at 50, 200, and 250 Hz are observed. In these tests the maximum spectral resolution of the technique is 10 kHz based on the data acquisition rate of 20 kHz. With further improvements it is possible to extend the data acquisition rate beyond the 20 kHz used here. Finally, Figs. 13 and 14 show the mean and rms concentration profiles at a further down-

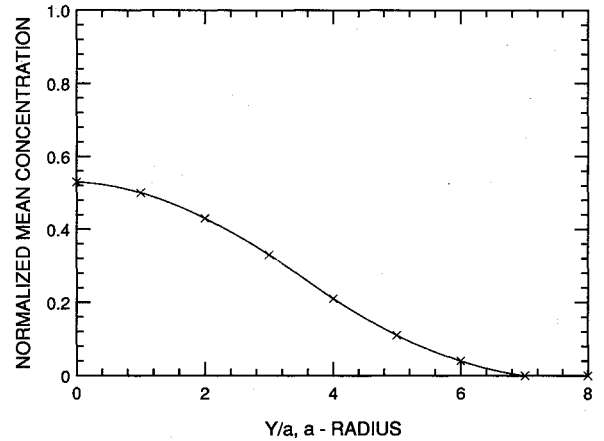


Fig. 13 Profile of mean fuel-air mixture fraction across a turbulent jet mixing in coflowing air at  $X/a = 20$ .

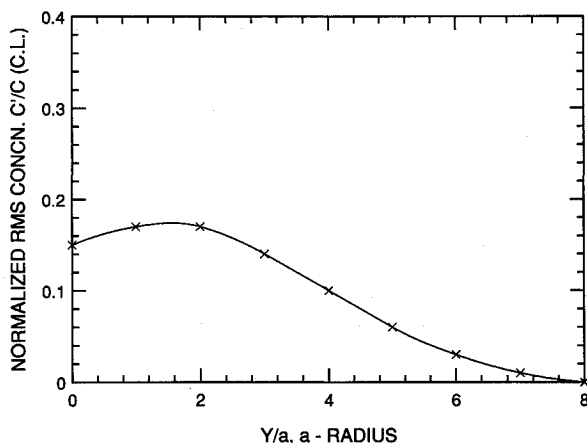
stream location of  $X/a = 20$ , where the fuel and air are fairly well mixed. At this location the mean and rms profiles are representative of well-developed jet profiles.

## V. Some Practical Issues

One of the important goals of this study was to identify and address the various issues that needed to be resolved in applying this technique to practical full-scale hardware at both atmospheric and higher pressures. In this section we address some of these issues in the context of practical implementation.

Table 1 Estimated capabilities of NO<sub>2</sub>-based LIF technique

Spatial resolution	0.75 × 0.75 × 2.0 mm (based on a 4.0-W laser)
Temporal resolution	50 μs (based on data acquisition rate of 20 kHz)
Spectral resolution	10 kHz (can be improved—related to above)
Sensitivity	10 ppm of NO <sub>2</sub> at atmospheric pressure
Linearity	0–5000 ppm at 1 atm 0–600 ppm at 4 atm 0–300 ppm at 10 atm
Dynamic range	>1:500 at 1 atm (1:30 at 10 atm—drops rapidly at higher pressures)
Upper pressure limit	15 atm (estimated)
Temperature limit	500 K (based on dissociation temperature of NO <sub>2</sub> <sup>7</sup> )
Effect of carrier gas	Diatomic molecule (such as N <sub>2</sub> , O <sub>2</sub> , H <sub>2</sub> )—no effect, signal varies linearly Larger molecule (such as CH <sub>4</sub> , CO <sub>2</sub> )—signal lower (33%), nonlinear Smaller molecule (such as He)—signal higher (30%), nonlinear

Fig. 14 Profile of rms variation of fuel-air mixture fraction across the turbulent jet mixing in coflowing air at  $X/a = 20$ .

#### A. Optical Access

Since this technique is based on frequency shifted fluorescence, optical windows can be used in practical tests if proper care is taken in their design. In the right-angle approach used here, optical access in three directions is required, viz., to allow the laser beam to enter and exit the test section and to collect the fluorescence signal in the normal direction. In the direction of propagation of the laser beam, relatively small size windows are adequate since the laser beam diameter is usually much smaller. Antireflection (AR)-coated quartz windows with the ability to withstand pressures of up to 30 atm are readily available commercially in this size. For the collection of the scattered fluorescence signal, a larger window is needed, but it can be of regular glass or optical quality quartz for high-pressure tests.

#### B. Scale of Tests

Based on the tests reported here, there appears to be no limit to the size of the test rig that can be used. For very long beam path and high seeding rates, self-absorption by NO<sub>2</sub> may become an issue. This limit remains to be investigated. Another potential problem with large scale tests is that since the collection lens has to be located far from the probe volume, the signal strength will degrade due to the reduced solid angle. Use of fiber optics can remedy this situation somewhat, but further work is required.

#### C. Effect of Carrier Gas

There is no effect of the carrier gas on the fluorescence signal as long as it is bimolecular. For larger sized molecules such as CO<sub>2</sub> or CH<sub>4</sub> (part of NG used in land-based combustors), the signal strength is lower (33%) because of increased quenching. This, however, does not represent a serious limitation in the use of methane as carrier gas because the relation between fluorescence signal and fuel fraction remains single-valued (albeit nonlinear), and can be directly

interpreted in terms of fuel-fraction. It should be noted that commercially NO<sub>2</sub> is available only in pure liquid form or in mixtures with N<sub>2</sub>, air, and inert gases such as helium and argon.

#### D. Limits on Temperature

The amount of preheating allowable in any mixing test using this technique is believed to be limited to 500 K because of rapid dissociation of NO<sub>2</sub> above this temperature. For this reason the technique cannot be used in combustor situations either as pointed out by Agarwal et al.<sup>7</sup>

#### E. Limits on Pressure

As results presented earlier in this article showed, the absolute upper limit of application of the technique appears to be 15-atm beyond which the dynamic range of the technique would be too small. Even at 10 atm, the dynamic range is reduced significantly because of increased quenching. An added complexity for pressures greater than atmosphere is that the fluorescence signal deviates from linear behavior, rendering its interpretation more difficult as was discussed earlier. Further work is needed to determine the exact cause for the nonlinearity.

#### F. Seeding of Fuel-Stream with Large Amount of NO<sub>2</sub>

An important practical issue in the seeding of large amounts of flow with NO<sub>2</sub> for application in full-scale atmospheric and/or subscale full pressure tests, where the flow rates are relatively high, is its reported toxicity. This issue is important because as reported by Matheson Gas Products<sup>11</sup> NO<sub>2</sub> is an extremely toxic gas. Extreme precautions are, therefore, required in the handling of the gas, including extensive monitoring of the test area to ensure safe operation. Extremely sensitive and reliable alarm systems for NO<sub>2</sub> are commercially available, but they tend to be fairly expensive. To avoid handling large numbers of NO<sub>2</sub> bottles for full-scale tests, NO<sub>2</sub> from high-concentration bottles could be introduced into the fuel-stream fairly upstream of the premixer before introduction into the premixer test section. This should permit safer operation of the system.

## VI. Conclusions

Laser-induced fluorescence technique based on NO<sub>2</sub> as marker has been studied extensively in laboratory-scale experiments at various operating conditions. Based on these results, it is shown that the technique can be successfully applied to study temporally resolved mixing in both full-scale atmospheric pressure hardware and small-scale high-pressure tests up to 15 atm. Currently, this technique is routinely used to quantify mixing performance of evolving premixer designs for screening purposes. The main advantage of the technique over conventional probe-sampling approaches is that unlike these techniques which yield only the mean fuel-fraction values, LIF can provide temporally resolved information about fluctuations in fuel-fraction values. Such fluctuations are believed to have significant impact on NO<sub>x</sub> emissions of the

combustor. In this study this capability was demonstrated by applying LIF to the study of mixing of a turbulent jet issuing into coflowing air. The technique has also been extended to higher pressures to determine the effect of pressure on quenching and on the sensitivity and linearity of the technique. Further work is required to determine the reason for nonlinear behavior of the fluorescence signal at elevated pressures. Similarly, more work is needed to determine the temperature limitation of the technique, though it is estimated to be 500 K based on the disassociation limit of NO<sub>2</sub>. To study mixing in combustor-type applications, other laser-based techniques, e.g., Raman scattering, would be more applicable.<sup>4</sup> The LIF technique can also be extended to obtain one- and two-dimensional images for flow visualization with further work. Table 1 summarizes the capabilities of the technique in detail based on the results obtained here.

### Acknowledgments

The authors would like to acknowledge the technical expertise of Frank Haller. Helpful technical discussions with Dominic Santavicca of the Pennsylvania State University, University Park, PA, are gratefully acknowledged.

### References

- <sup>1</sup>Fenimore, C. P., "Chemistry in Premixed Flames," MacMillan, New York, 1964.
- <sup>2</sup>Leonard, G., and Correa, S., "NO<sub>x</sub> Formation in Premixed High Pressure Lean Methane Flames," 2nd ASME Fossil Fuels Combustion Symposium, New Orleans, LA, Jan. 1990; see also Singh, S. N. (ed.), ASME/PD, Vol. 30, 1990, pp. 69-74.
- <sup>3</sup>Eckbreth, A. C., "Laser Diagnostics for Combustion, Temperature and Species," *Energy and Engineering Science Series*, edited by A. K. Gupta and D. G. Lilley, Abacus Press, Cambridge, 1988.
- <sup>4</sup>Gulati, A., and Correa, S., "Raman/LV Measurements in a CO/H<sub>2</sub>/N<sub>2</sub> Flame at High Reynolds Number," AIAA Paper 89-0056, Jan. 1989.
- <sup>5</sup>Correa, S. M., and Warren, R. E., "Supersonic Sudden-Expansion Flow with Fluid Injection: An Experimental and Computational Study," AIAA Paper 89-0389, Jan. 1989.
- <sup>6</sup>McDaniel, J. C., and Graves, J., Jr., "A Laser-Induced Fluorescence Visualization of Traverse Sonic Fuel Injection in a Non-Reacting Supersonic Combustor," AIAA Paper 86-0507, Jan. 1986.
- <sup>7</sup>Agarwal, Y., Hadeishi, T., and Robben, F., "Measurement of NO<sub>2</sub> Concentration in Combustion Using Fluorescence Excited by an Argon-Ion Laser," AIAA Paper 76-136, Jan. 1976.
- <sup>8</sup>Lozano, A., "Laser-Excited Luminescent Tracers for Planar Concentration Measurements in Gaseous Jets," Ph.D. Dissertation, Stanford Univ., Stanford, CA, 1992.
- <sup>9</sup>Myers, G. H., Silver, D. M., and Kaufman, F., "Quenching of NO<sub>2</sub> Fluorescence," *Journal of Chemical Physics*, Vol. 44, No. 2, 1966, pp. 718-723.
- <sup>10</sup>Tennekes, H., and Lumley, J. L., *A First Course in Turbulence*, MIT Press, Cambridge, MA, 1972.
- <sup>11</sup>Braker, W., and Mossman, A. L., "Effects of Exposure to Toxic Gases—First Aid and Medical Treatment," Matheson Gas Products Co., Newark, NJ, 1970.

Recommended Reading from Progress in Astronautics and Aeronautics

## High-Speed Flight Propulsion Systems

S.N.B. Murthy and E.T. Curran, editors

This new text provides a cohesive treatment of the complex issues in high speed propulsion as well as introductions to the current capabilities for addressing several fundamental aspects of high-speed vehicle propulsion development. Nine chapters cover Energy Analysis of High-Speed Flight Systems; Turbulent Mixing in Supersonic Combustion Systems; Facility Requirements for Hypersonic Propulsion System Testing; and more. Includes more than 380 references, 290 figures and tables, and 185 equations.

1991, 537 pp, illus, Hardback  
ISBN 1-56347-011-X  
AIAA Members \$54.95  
Nonmembers \$86.95  
Order #: V-137 (830)

Place your order today! Call 1-800/682-AIAA



American Institute of Aeronautics and Astronautics

Publications Customer Service, 9 Jay Gould Ct., P.O. Box 753, Waldorf, MD 20604  
FAX 301/843-0159 Phone 1-800/682-2422 9 a.m. - 5 p.m. Eastern

Sales Tax: CA residents, 8.25%; DC, 6%. For shipping and handling add \$4.75 for 1-4 books (call for rates for higher quantities). Orders under \$100.00 must be prepaid. Foreign orders must be prepaid and include a \$20.00 postal surcharge. Please allow 4 weeks for delivery. Prices are subject to change without notice. Returns will be accepted within 30 days. Non-U.S. residents are responsible for payment of any taxes required by their government.